Supporting Information for

Arctic freeboard and snow depth from near-coincident CryoSat-2 and ICESat-2 (CRYO2ICE) observations: A first examination of winter sea ice during 2020-2022

Renée Mie Fredensborg Hansen[1,2,3], Henriette Skourup[1], Eero Rinne[2], Knut Vilhelm Høyland[3], Jack Christopher Landy[4], Ioanna Merkouriadi[5] and René Forsberg[1]

[1]DTU Space, Department of Geodesy and Earth Observation, Elektrovej Building 327, 2800 Kgs. Lyngby, Denmark

[2]The University Centre in Svalbard (UNIS), Department of Arctic Geophysics, P.O. Box 156, 9171 Longyearbyen, Norway

[3]Norwegian University of Science and Technology (NTNU), Department of Civil and Environmental Engineering, S. P. Andersens veg 5, 7031 Trondheim, Norway

[4]The Arctic University of Norway (UiT), Department of Physics and Technology, PO Box 6050 Langnes, 9037 Tromsø, Norway

[5]Arctic Research Centre, Finnish Meteorological Institute, P.O. Box 503, 00101 Helsinki, Finland

Contents of this file

Text S1 to S8
Figures S1 to S6
Tables S1

Introduction

This supplement contains text, figures, and tables in support of the main document.

Text S1 describes the pre-processing steps applied to CryoSat-2 along with the methodology used to identify corresponding LARM, CCI+ , AMSR2 and SMLG observations.

Text S2 presents the data binning methodology used to bin ICESat-2 to CryoSat-2 observations (to achieve CRYO2ICE observations). Here, a sensitivity analysis of the search radius is presented.

Figure S1 presents the sensitivity analysis as a function of search radius, where we have investigated number of ICESat-2 points available per search radius and the variance between the points (inspired by semi-variograms).

Text S3 presents all the reference observations identified for this period of study, along with analysis conducted showcasing how these reference observations were not possible to compare with.

Text S4 describes additional snow depth reference observations identified and how they were not possible to be used in this study.

Figure S2 shows the identified shipborne reference observations for the period of study for any available ship observations along with snow depth estimations from ship, overlaid with the CRYO2ICE observations to identify coincidence.

Text S5 discusses the acoustic snow depth buoys from the Alfred-Wegener-Institute (AWI) and how the raw data vs filtered data (what is used in the study) appear, and what may impact the sensors to provide high snow accumulation estimates.

Figure S3 shows the raw and filtered observations of the AWI snow depth buoys to support Text S5.

Figure S4 shows the comparison with in situ reference observations identified in Text S3.

Text S6 described the comparison presented in Figure S4 to reference observations.

Text S7 discusses a comparison made to each individual SIMBA buoy. Here, we discuss how the fact that the buoys were deployed on different types of ice (ridge or level ice) may impact the snow accumulation observed by the buoy.

Figure S5 shows the snow depth estimates for each individual SIMBA buoy to support Text S7.

Table S1 presents statistics for comparison with the individual SIMBA buoys.

Text S8 discusses the uncertainty of snow density (the only parameter to change besides the freeboard estimates of ICESat-2 and CryoSat-2).

Figure S6 supports Text S8 with a snow density/snow depth simulation to present the impact of using constant or time-varying snow densities, both which have been used in former altimetry studies.

Text S1. Pre-processing of CryoSat-2 data and finding corresponding LARM/CCI+ observations along with AMSR2 and SMLG observations

We further pre-process the CryoSat-2 Baseline-E freeboard data by removing points where one or more of the following error-flags (available in the following parameter: *flag_prod_status_20_ku* were activated: *calibration_warning, sarin_bad_velocity, sarin_out_of_range, sarin_bad_baseline, delta_time_error, mispointing_error, sarin_side_redundant, sarin_rx_2_error, sarin_rx_1_error, sarin_height_ambigous, surf_type_class_ocean, freeboard_error, peakiness_error, ssha_interp_error, orbit_discontinuity, orbit_error* and *height_sea_ice_error*. Furthermore, the surface type flag that identifies the observation as sea ice (*surf_type_class_sea_ice)* is also activated. While the interferometric SAR (SARIn) flags are only activated in the SARIn mode (primarily active over surfaces with steep slopes such as coastal regions, ice sheet margins etc.), we still include these error flags in case this analysis should be performed over SARIn data. Based on investigation of four specific tracks from March 2021, between 38-61\% of data is filtered away using these error flags, which also results in erroneous freeboard values being filtered (e.g., large negative freeboards).

We also extract the snow depth from Warren et al. (1999) (noted as W99 hereon after) and find the closest points along the 20Hz sampling of CryoSat-2 freeboards (W99 given at 1 Hz). This is for comparison later on in terms of growth rates based on observations (compared with models) but it is important to highlight that W99 is based on observations from 1950-1990s and therefore may not be as comparable to today's results, especially in terms of magnitude of snow depths.

For LARM, the product is available per trajectory, and provides amongst other the radar freeboard as well as latitude, longitude, and time. Here, we extract LARM CryoSat-2 freeboards, latitudes, and longitudes from the same day as the Baseline-E reference track (using CryoSat-2's start of acquisition time as reference). The reference time is used as selection criteria when extracting freeboard observations in the LARM product along with the in-product flag that states whether the point originates from floes ("Sea_Ice_Class = 1"). Of the extracted freeboards from the corresponding day, the latitudes and longitudes are collocated with Baseline-E observations and kept if they agree within five decimals accuracy.

For CCI+, the observations are provided as trajectories pr. month (a L2P product). The monthly product is not provided with any type of orbit ID to select by; however, the time of acquisition, latitude and longitude is included in the product. We use the latitude and longitude at five decimals accuracy, as well as the time parameter (extracted as 'YYYY-MM-DD HH:MM:SS.SSSSSS' at microseconds accuracy) for collocation with the Baseline-E CryoSat-2 observations as reference. However, the CCI+ product provides time in the format of Universal Time Coordinate (UTC) whereas ESA's Baseline-E provides time in the format of International Atomic Time (TAI). Currently (as of January 2023) TAI is 37 seconds ahead of UTC time due to leap seconds which is accounted for when collocating the CryoSat-2 observations.

For SMLG, we extract the snow depth and coordinates of the SMLG from the same day as the CRYO2ICE track flew. The SMLG is provided as Cartesian coordinates (X, Y),

which are projected onto the polar stereographic map and the nearest-neighbouring point to the CRYO2ICE observations are extracted.

Text S2: Data binning of ICESat-2 to be comparable with CryoSat-2 (CRYO2ICE binning)

Based on a sensitivity analysis of one month of CRYO2ICE tracks presented in Figure S1, we investigate the variance of the difference between the radar freeboards at each bin point at different search radii. We use the variance between ICESat-2 and CryoSat-2 freeboards as a measure of spatial variability and investigate how large an impact there will be by using a larger search radius - this is similar to a semi-variogram analysis; however, we do not check the variance across all potential distances with every subsequent point. Instead, we focus only on how the freeboards are of similar variance depending on the search radius. We would expect a larger variance with small search radii, as they will be less impacted by the number of points compared to that of a larger search radius. A similar variance of the differences in freeboard are seen across most of the search radii (with only a few outliers) as shown in Figure S1a.

Since we aim to keep the highest possible spatial resolution (at CryoSat-2 footprint), we aim to get the largest search radius (to include as much data as possible) where spatial variability is still present (expecting it to be more representative rather than including points even further away from the CryoSat-2 footprint). Since the variance is similar across all search radii between 0 to 3500 m, we expect this data to provide similar results. However, what is noticeable is the amount of additional data points gained by introducing a larger search radius (Figure S1b). We use 3500 m radius as the maximum, since the distance between ICESat-2 beam pairs are 3300 m, and this will allow us to include points from all three beams if the orbits of ICESat-2 and CryoSat-2 are almost completely aligned. However, we note that the alignment is not perfect and that only at specific points along the tracks would the orbits be considered almost fully near-coincident. To take this into account, we make use of the search radius of 3500 m instead of 3300 m.

We also note that we did compute a semi-variogram analysis for all the tracks in the month of November, but there was no consensus regarding use of search radii (no convergence) due to the incomplete and inconsistent data coverage of the CRYO2ICE tracks. Based on these analyses, we select a search radius large enough to ensure enough data to compare with and apply inverse-distance-weighting to ensure that observations closest to the reference points are prioritized.
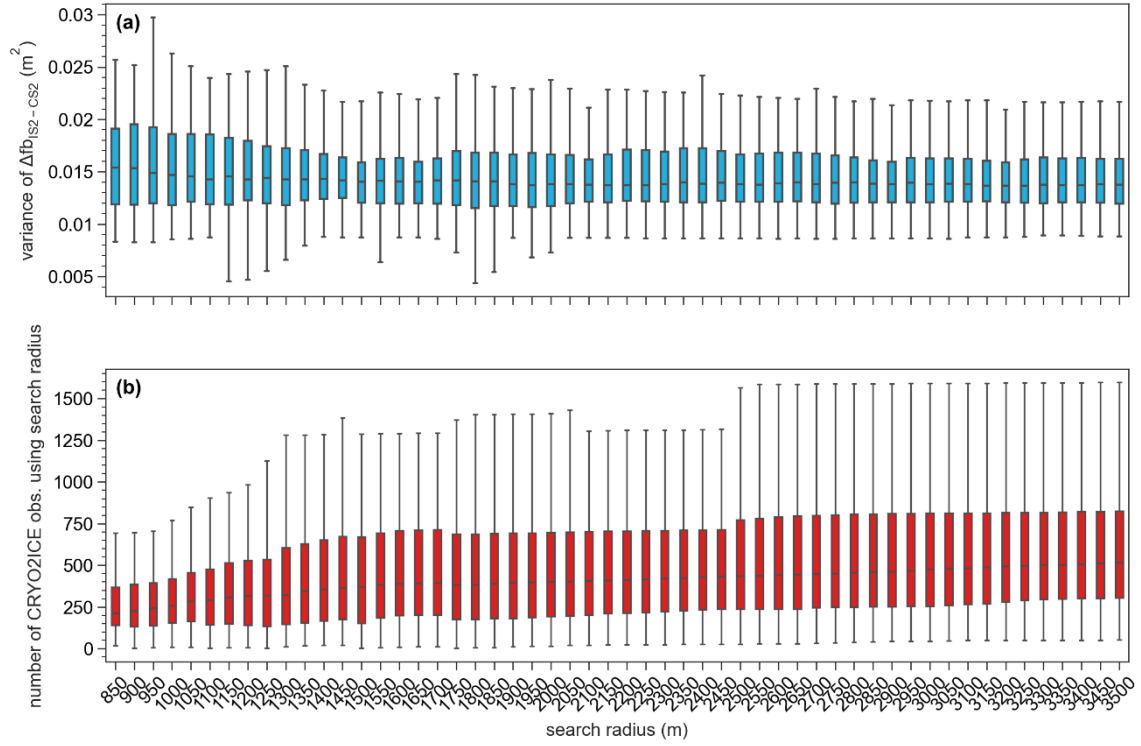
Figure S1. Variance between CryoSat-2 (CS2) and ICESat-2 (IS2) freeboards as a function of search radius (76 track considered, from 2nd of November until 13th of December), as well as number of points as a function of search radius. Outliers are not shown.

Text S3: In situ reference measurements to compare with

There were no successful Arctic airborne campaigns dedicated to the C2I campaign during the period of the study (primarily due to COVID-19), and due to the sparse coverage of C2I orbits, the quantity of available reference measurements are limited (see Text S2 for discussion on available reference observations). However, both seasonal ice mass balance (SIMBAs) and acoustic snow depth buoys were deployed during the final leg of the MOSAiC (Multidisciplinary drifting Observatory for the Study of Arctic Climate) expedition, and we shall utilise observations from these for a comparison. The acoustic buoys deployed by the Alfred Wegener Institute (AWI) consist of four ultrasonic sensors, which each measures its distance from the snow's surface. It is therefore not the actual snow depth that the sensors measure, but instead the accumulation and ablation of the snow surface relative to the initial snow depth, that is converted to snow depth (Nicolaus et al., 2021).

In total, we identified five acoustic buoys (deployment reports available on Grosfeld et al. (2016, last access: 2023/05/12): 2020S98, 2020S105, 2020S106, 2020S107, and 2020S108, but only three of the buoys (2020S108, 2020S106, and 2020S105) had coincident snow depth measurements with our C2I study period.

In addition, several SIMBA buoys were deployed. While not currently published, snow depth estimates from two of the buoys were provided for this study by the contact persons listed in Grosfeld et al. (2016). FMI0607 (also noted as 2020T84) was deployed on level first-year sea ice with initial thickness of 1.14 m and snow depth of 0.03 m. PRIC0906 (or 2020T85) was deployed on a ridge where sea ice thickness was $>$4 m with initial snow depth of 0.05 m. Both buoys carried a thermistor-string frozen into the sea ice. From the changes in the vertical temperature profile, the location of air-snow, snow-ice and ice-water interfaces can be estimated, providing information of the snow depth and ice thickness (Jackson et al., 2013; Liao et al., 2019).

When comparing with reference observations, the buoy observations are first post-processed to daily snow depth estimates at the average daily location. We identify comparable C2I points assuming they are within +/- 50 km and 2 days of the buoy locations and acquisition time following Ricker et al. (2015).

Text S4: Additional snow depth reference observations comparisons with CRYO2ICE-derived snow depth estimates

Due to the limited reference observations of snow depth on sea ice available, we have investigated potential other data sources than the buoys presented in Section 3.2. During winter 2021-2022, the CryoSat Validation Experiment (CryoVEx) CRYO2ICE 2022 campaign, lead by DTU Space, took place from 21 March 2022 through 14 April 2022. However, when the campaign journeyed towards Station Nord to conduct dedicated CRYO2ICE under-flights, ICESat-2 went into safe-hold mode for the duration of the remaining campaign (4 April through 12 April, https://icesat-2.gsfc.nasa.gov/science/specs, last access: 2022/10/26), cutting the campaign short (till 7 April 2022). The safe-hold mode resulted in no dedicated airborne CRYO2ICE validation data during the winter season of the CRYO2ICE Arctic period (summer 2020 until

summer 2022). While there were no airborne campaigns flown during the period of the study (neither Operation IceBridge, CryoVEx nor AWI's IceBird campaigns were flown), ship campaigns were conducted.

We investigated the Ice Watch Current and Archive Ice Observations Version 1 (NSIDC-0705) product, available on https://nsidc.org/data/nsidc-0705/versions/1 (last access: 2023/02/13). This product is an open-source forum for sharing shipborne Arctic sea ice observations data, where the ships utilise the ASSIST (Arctic Shipborne Sea Ice Standardization Tool) software to record ship tracks and sea ice conditions throughout the Arctic Ocean. For the period of the study (November 2020--April 2021), we identified the following three cruises where ship borne observations were available (from the connecting website https://icewatch.gina.alaska.edu/, last access: 2023/02/16).

- KV Svalbard (2020-10-15 to 2020-11-25) denoted ASSIST#1,
- R/V Kronprins Haakon (2021-02-09 to 2021-02-28) denoted ASSIST#2,
- and R/V Kronprins Haakon (2021-03-02 to 2021-03-24) denoted ASSIST#3.

The observations are divided into three ice types: primary, secondary, and tertiary, and for each ice type, the snow depth is determined. We have for each point computed the average snow depth from all three ice types, which provides one snow depth observation across all ice denoted by the observers on the ship.

In total, 357 observations were obtained by the three ship campaigns during the winter season 2020-2021, however only 141 of these included snow depth estimates (ASSIST#1: 72 observations, ASSIST#2: 54, and ASSIST#3: 16). The coverage of all observations of the three campaigns, as well as observations on registered snow depth estimates are presented in Figure S2. It is noteworthy that the two campaigns with most observations of snow available are located east of Svalbard, where we have very limited CRYO2ICE observations. Furthermore, ASSIST#3 that covers significantly more of the Arctic Ocean only have 16 snow depth observations throughout the cruise.

To make a comparison, we conduct the same analysis as with the buoys presented in Section 3.2. However, we note that even with a maximum distance of 100 km from the ship observations as well as a temporal latency of +/- 15 days, only one point could be compared with CRYO2ICE observations based on those conditions. Therefore, it was not possible to conduct a comparison with ASSIST data. It is however noteworthy, that average snow depths observed by the three campaigns were. 10 cm, 6 cm and 7 cm, for ASSIST#1-3, respectively, with standard deviations ranging between 2-5 cm. Maximum snow depth observed ranged between 10-20 cm for all the campaigns, highlighting the limitations of comparing with ship observations due to their routes predominantly traversing through thin, non-deformed ice for accessibility and safety.

Beyond the identified AWI snow depth buoys presented in Section 3.2, we also investigated whether other snow depth buoys were available. In addition to AWI's snow depth buoys, three additional coordinated buoy activities for snow depth estimates on sea ice is available: (a) The Cold Regions Research and Engineering Laboratory (CRREL)-Dartmouth Mass Balance Buoy Program (Perovich et al., 2023) where ice mass balance buoys (IMBs) are deployed; (b) Scottish Association for Marine Science (SAMS) IMBs, often denoted as SIMBA buoys, which are deployed by various institutes; and (c) ICE-T buoys, primarily deployed by Locean (under the project OPTIMISM,

, last access: 2023/02/15). They are all thermistor-string buoys, where the snow depth estimate is determined from the temperature measurements of the string. Sometimes the buoys may be equipped with additional sensors to observe other meteorological variables or geophysical variables.

During the period of study, there were no active CRREL-Dartmouth IMBs: their most recent IMBs ended its data transmission in 2018 (according to http://imb-crrel-dartmouth.org/live-data/, last access: 2023/02/15). There were also no ICE-T buoys available during the period in question. Of publicly available ICE-T are currently four from the years: 2013, 2014, 2015, and 2018 (Vivier and Lourenco, 2023) on SEANOE (https://www.seanoe.org/data/00766/87766/, last access: 2023/02/16). Of SIMBA buoys, we identified four buoys that were active during the period of the study: 2020T78 (2020/08/23 to 2021/02/26), 2020T81 (2020/08/30 to 2021/02/10), 2020T84 (2020/08/26 to 2021/06/02), and 2020T85 (2020/09/19 to 2021/07/09). These buoys were deployed during the MOSAiC expedition (https://mosaic-expedition.org/, last access: 2023/02/15). Currently, the post-processed data with snow depth and sea ice thickness determined from the temperatures are not public. Only the buoys with end dates in 2020 have been processed and published (Lei et al., 2021). We contacted the contact persons of the four SIMBA buoys as denoted on AWI's website, where two buoys were available with data acquired during the winter season of 2020-2021: a comparison with these observations are provided in Section 3.2.
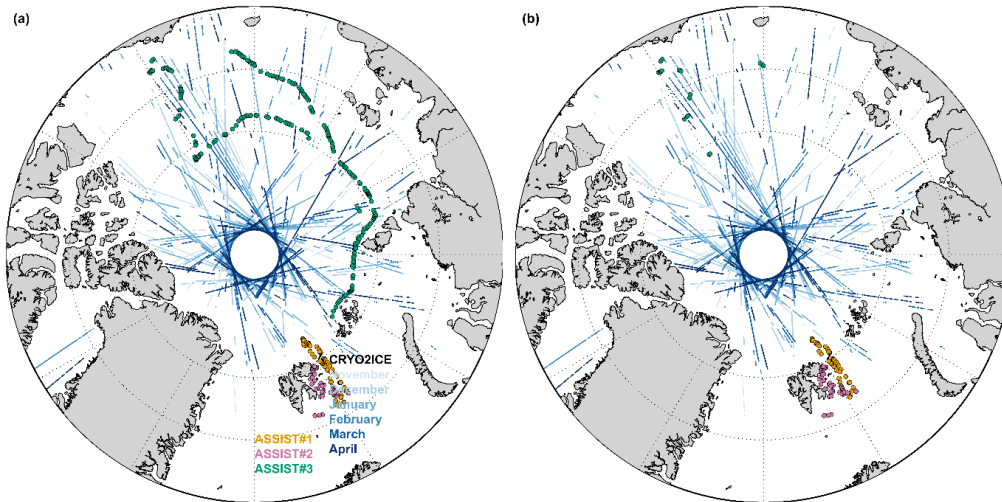

Figure S2. ASSIST ship borne observations during the three campaigns of the winter season 2020-2021. (a) locations of all ship observations provided for each campaign in ASSIST, (b) the locations of available snow depth observations for all three campaigns

Text S5: Raw and filtered data from AWI snow depths

The acoustic AWI snow depth buoys are filtered based on various requirements presented in Nicolaus et al. (2021). Figure S3 shows the unfiltered ('RAW') observations along with the filtered data for all four sensors of each of the five acoustic buoys of relevance to this study.

Here, sensors routinely observe distances to initial snow depth (later to be converted into snow depth) that are mixed and often inconclusive, and some are even of the height of the sensor itself. It appears that for several of the sensors, snow might accumulate around – or even on – the sensors, which impacts the snow depth estimates.

While the filtration scheme appears to work reasonably well to extract a snow depth estimate, it also suggests that the buoys are limited in data if heavy precipitation events occur as it impacts the sensors. If snow accumulates around the sensor, the sensor will observe higher snow depths than what is the case for the surrounding sea ice – and to what we will observe from satellites.

As such, this might explain why the acoustic sensors observed higher snow depths than the satellites. Especially, since all sensors were deployed around the same area and drifting in a similar pattern, it is likely that they were all affected by a similar precipitation event which impacted the sensors as snow accumulated around it.

To the best of our knowledge, the AWI snow depth buoy estimates for the winter season 2020-2021 has not been compared with other snow depth estimates. However, Nicolaus et al. (2021) do note that for their entire dataset, they noted a total accumulation of 30.5 cm, which is less than the snow depth estimates of ~70 cm. We therefore conclude that these snow depth estimates are not reasonable. Nicolaus et al. (2021) further note that Arctic snow depth buoy estimates from the acoustic buoys have larger uncertainties due to the higher occurrence of noise in the Arctic. The noise is likely related to enhanced frosting on the sensor and buoy structure due to higher air humidity. They also note that the large scatter is a result from drifting/blowing snow, snow fall, and instrument icing resulting in apparently higher surfaces.
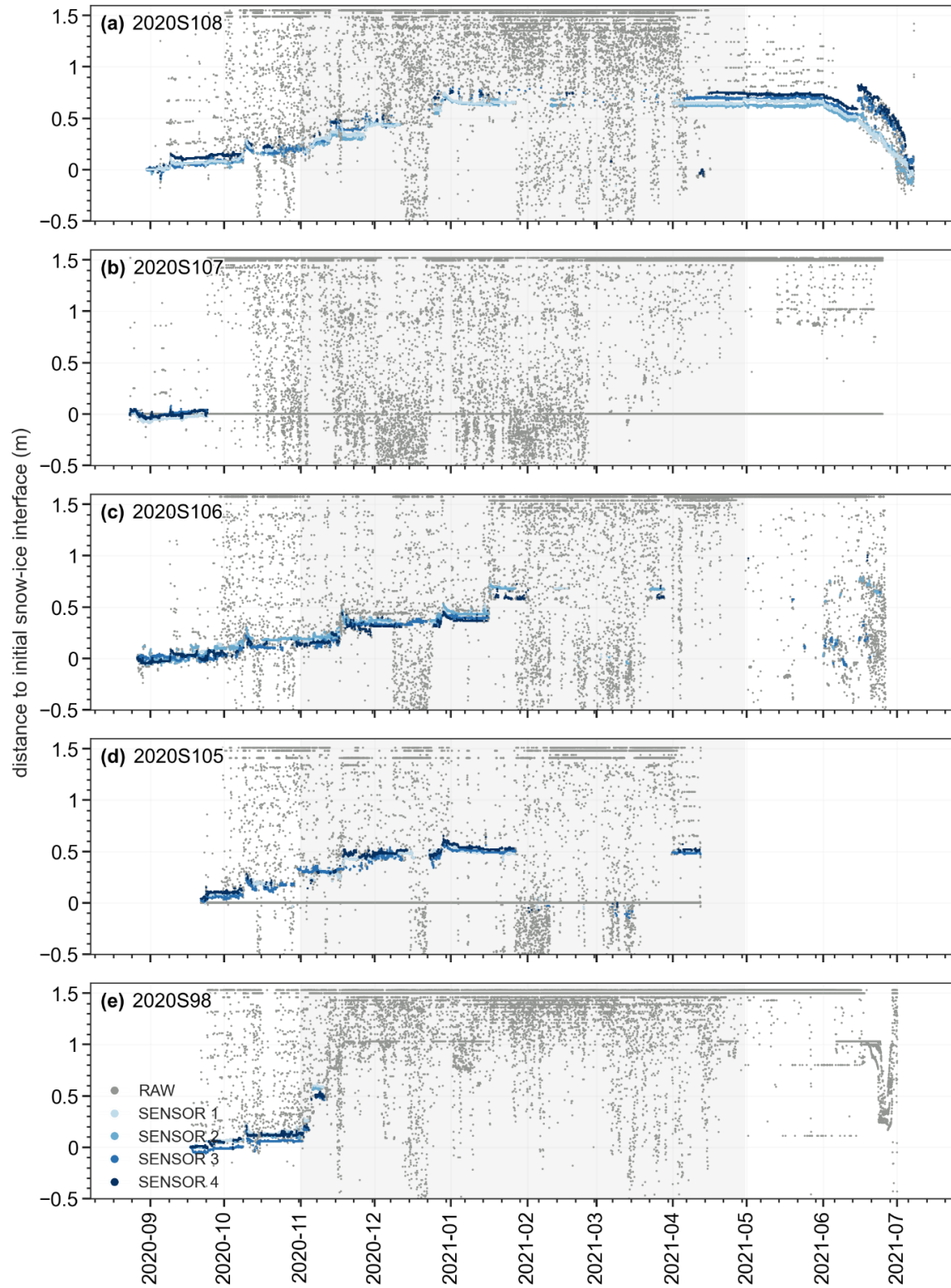
Figure S3. Observations available from the identified AWI buoys 2020S98, 2020S105, 2020S106, 2020S107, and 2020S108. We here highlight the processed observations from each of the four sensors, as well as the raw (but filtered) data not included in the processed product. Grey area denotes the winter season 2020-2021.
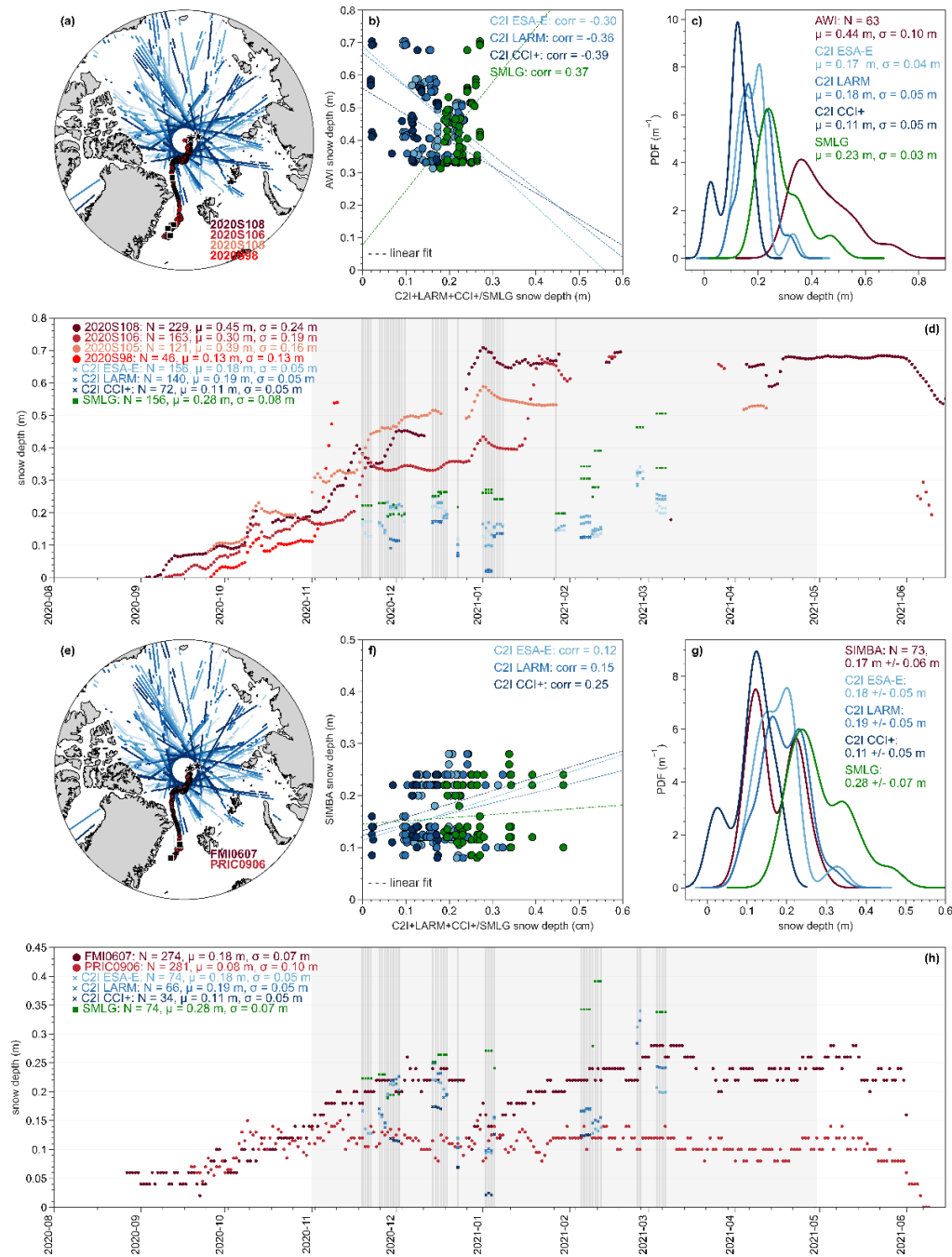
Figure S4. Comparison against Alfred Wegener Institute (AWI) and Seasonal Ice Mass Balance Array (SIMBA) snow depth buoys. (a) location of buoys overlaid C2I 2020-2021 tracks (Nov-Apr). (b) comparison between coincident buoy and C2I/SMLG snow depths (within +/- 50 km and 2 days). (c) distribution of coincident snow depth observations. (d) full time-series of snow depths from coincident buoy/C2I/SMLG observations. Grey lines indicate coincident observations. There was no overlap between the buoys and AMSR2 observations. (e-h) same as (a-d) for SIMBA buoys.

Text S6: Comparison between C2I snow depths observations and other basin-scale estimates with in situ reference measurements

In situ observations of snow depth on sea ice are scarce, but buoys (acoustic and thermistor string) were identified for the period of 2020-2021 (Section 2.3.2). Here, we observe for the acoustic buoys (Figure S4a-d) significant accumulation of snow that is not reflected in the C2I or model estimates. Overall, the acoustic buoys show snow depth values up to 0.70 m, with averages of 0.30-0.45 m across the entire acquisition period. For coincident C2I points, the average buoy snow depth is 0.44 m where the C2I ranges between 0.11-0.19 m and SMLG estimates 0.28 m. The periods of rapid increase in acoustic buoy snow depth, in November 2020 and January 2021, elevate the in situ snow depth well above the satellite and model estimates. The higher snow depths from these buoys are likely caused by snow accumulation around and on the sensors (see Figure S3 and Text S5), leading to a potential overestimation of the in situ recorded snow depth. Such rapid increases have been observed previously (Nicolaus et al., 2021}; however, we cannot be sure these measurements are unrealistic on floe scales.

The SIMBA buoys (Figure S4e-h) show more comparable snow depth accumulation patterns to the satellite and model-based estimates. It is worth noting that PRIC0906 was deployed on a ridge, which will result in a different accumulation pattern than expected on level sea ice. Here, the top of ridges is likely to experience thinner snow depth due to wind re-distribution (Liston et al., 2018) with the wind/blown snow accumulating around the ridges in sheltered areas causing deformed ice to have thicker snow depths (Sturm et al., 2002). The statistics provided in Figure S4f includes both SIMBA buoys, but individual comparisons are provided in Text S7, Figure S5 and Table S1, to fully investigate how well they compare as the individual buoys might represent different aspects. To fully examine the capabilities of C2I snow depth retrieval, it is necessary to compare with near-coincident reference observations distributed over time and space, preferably from airborne or ground-based campaigns with similar instruments. That will be the aim of future work, when the CRYO2ICE Antarctic under-flight, conducted on the 13th of December 2022 as part of the ESA Cryo2IceEx/NERC DEFIANT campaign, will be investigated.

Text S7: Comparison to individual SIMBA buoys

       In addition to an overall comparison with both buoys simultaneously as provided in Figure S4, we also compare individually because the buoys were deployed in different settings and observe much different accumulation patterns. From Figure S5 and Table S1 we can observe that the SIMBA buoy deployed on level ice (FMI0607) shows similar patterns as the satellite observations, although with C2I observations generally lower. SMLG is much higher than the SIMBA buoy, but the more recent version of SMLG shows more reasonable results.

       Correlations of 0.66-0.71 were observed for C2I observations compared with FMI0607. SMLG and mW99 had the weakest correlation observed between the observations compared (with mW99 having a correlation of -0.12). SMLG also observes higher snow depth in general. Generally, snow depth estimates from satellites on pan-Arctic scales have shown low-to-moderate correlations when compared to buoys (Zhou et al., 2020), even at daily scales, so these results from C2I are promising. However, to fully evaluate the accuracy and capability of C2I snow depth estimates (and future CRISTAL estimates) at orbit-based segments, further analysis with airborne campaigns is necessary. We aim, for future work, to investigate the CRYO2ICE Antarctic under-flight conducted on December 13th, 2022, where several sensors (laser, Ku/Ka, and snow radar) were carried along. While Antarctic sea ice is a different type of ice, this will be the first possibility to fully evaluate the C2I observations with airborne observations, and along the entirety of the track.
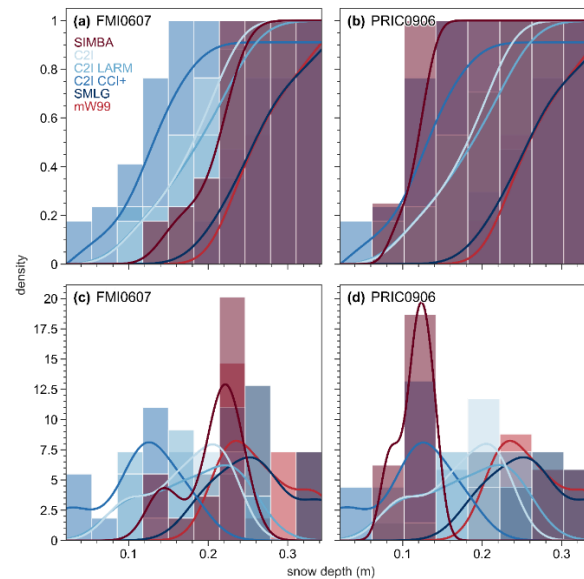

Figure S5. Snow depth estimates from SIMBA buoys (FMI0607, PRIC0906) compared with near-coincident (+/- 50 km and 2 days) C2I, reanalysis-based and climatology estimates. (a-b) shows the cumulative distribution and (c-d) the distribution of snow depth estimates for all the observations. We note that FMI0607 was deployed on level ice, whereas PRIC0906 was deployed on a pressure ridge.

Table S1. Statistics of comparison between individual SIMBA buoys and the snow depth estimates. Rows are coloured by method of snow depth estimation: blue – CRYO2ICE, green – reanalysis-based, and orange – climatology of in situ observations from 1950-1990s.

	Correlation		RMSD (m)		Slope		Intercept		Mean + st.dev. (m)		Bias: buoy-est. (m)	
	FMI0607	PRIC0906	FMI0607	PRIC0906	FMI0607	PRIC0906	FMI0607	PRIC0906	FMI0607	PRIC0906	FMI0607	PRIC0906
Buoy	--	--	--	--	--	--	--	--	0.20 ± 0.04	0.12 ± 0.02	--	--
C2I ESA-E	0.71	0.05	0.04	0.08	0.53	0.02	0.11	0.11	0.17 ± 0.05	0.17 ± 0.05	0.03	-0.05
C2I LARM	0.66	0.01	0.05	0.08	0.42	0.00	0.13	0.12	0.18 ± 0.06	0.18 ± 0.06	0.02	-0.07
C2I CCI+	0.74	-0.04	0.09	0.06	0.51	-0.02	0.15	0.12	0.12 ± 0.05	0.11 ± 0.05	0.09	0.00
SMLG	0.12	-0.17	0.08	0.15	0.08	-0.06	0.18	0.13	0.26 ± 0.05	0.26 ± 0.05	-0.06	0.15
mW99	-0.12	0.14	0.09	0.14	-0.09	0.06	0.23	0.10	0.27 ± 0.05	0.26 ± 0.04	-0.06	0.15

Text S8: Uncertainty of snow depth estimation – snow density simulation

We investigate the difference in snow depth between choosing a constant snow density (as we have used for this study, at 300 kg/m^3) and deriving snow depth using a time varying snow density estimate using either 250-450 kg/m^3 (based on the observations of Tonboe et al. (2010), Warren et al. (1999) and King et al. (2020)) or the density range given by Mallet et al., (2020), see Figure S6. Here, for the large density range observed in other studies, we see a density uncertainty (compared to using a constant snow density) of 4 cm. Using the more commonly used snow density range of Mallet et al. (2020), we observe a density uncertainty of approximately 1 cm. Thus, highlighting that the snow depth estimates are less affected by the snow density estimates. The overall uncertainty of the snow depth estimates will thus rely heavily on the provided freeboard estimates, which currently are not provided in the products used in this study.
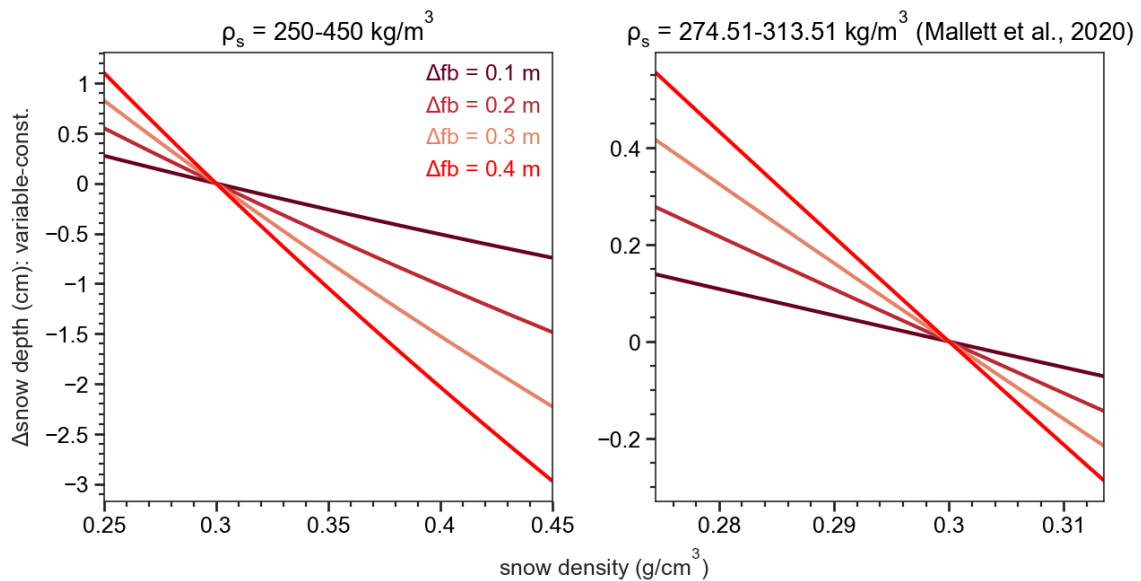

Figure S6. Investigating of impact on using a varying or constant snow density estimate to derive CRYO2ICE snow depths based on differences in freeboards (Δfb is the difference in freeboard between ICESat-2 and CryoSat-2.